SUBHARMONIC GENERATION IN AN ACOUSTIC FABRY-PEROT INTERFEROMETER

Thesis for the Degree of M. S.
MICHIGAN STATE UNIVERSITY
JACK A. BAMBERG
1967

ABSTRACT

SUBHARMONIC GENERATION IN AN
ACOUSTIC FABRY-PEROT INTERFEROMETER

by Jack A. Bamberg

Above a certain energy density threshold in an intense ultrasonic standing wave, subharmonics of the driving frequency are sometimes present. To study this effect, an acoustic Fabry-Perot interferometer was constructed, consisting of two air-backed quartz transducers submerged in water. One of the transducers is driven at frequencies around its 3 MHz resonance. Electronic analysis of the waveforms present in the cavity is accomplished with a spectrum analyser connected to the other quartz transducer. Optical methods are used as a supplementary means of analysis.

It was observed that subharmonics exist only at frequencies for which the cavity is in resonance and always occur in pairs, such that the sum of their frequencies is equal to the driving frequency. These discrete frequencies appear only in regions near integral submultiples of the driving frequency. The pressure in the cavity at the onset of subharmonic oscillation may be as low as 1.5 atmosphere. In this study, subharmonics were obtained only when the cavity reflector had a frequency dependent reflection coefficient.

SUBHARMONIC GENERATION IN AN ACOUSTIC FABRY-PEROT INTERFEROMETER

by

Jack A. Bamberg

A THESIS

Submitted to
Michigan State University
in partial fulfillment of the requirements
for the degree of

MASTER OF SCIENCE

Department of Physics

1967

ACKNOWLEDGMENT

The author wishes to express his gratitude to Professor E. A. Hiedemann and Dr. B. D. Cook for the assistance received in the formulation and solution of this problem. The discussions with Dr. W. R. Klein, Dr. F. Ingenito, and the other members of the ultrasonics group at Michigan State University also have been very helpful. The financial support of the Office of Naval Research is gratefully acknowledged.

TABLE OF CONTENTS

LIST OF TABLES

LIST OF FIGURES

Figure | Page

CHAPTER I

INTRODUCTION

It is sometimes possible to solve problems in acoustics by the elimination of nonlinearities in the equations describing the system; this approximation often leads to valuable information about the system. However, there are also many systems for which linear treatments will not suffice. For example, the deviation from a linear Hooke's Law relationship becomes significant when large amplitude vibrations occur in an elastic medium.

A more accurate description may be obtained in such instances, by including a few nonlinear terms as perturbations on the linear situation. In other cases, new phenomena occur in a nonlinear system which can not occur in a linear system. An example of this type is the occurrence of oscillations at a lower frequency than the resonant frequency of the system, i.e. subharmonics. The above approximate techniques are not useful here, since the effect depends upon the very terms we need to neglect. It is difficult to treat such problems analytically.

The existence of subharmonics has long been known; the subject was discussed as early as 1877 by Lord Rayleigh [1]. Since then, numerous examples have appeared in the literature. Most of these exhibit a mechanical nonlinearity leading to an equation of motion of the form

$$m\ddot{x} + c\dot{x} + f(x) = F(\omega t) \qquad (1.1)$$

where x is the vibration amplitude, F is the external driving force, m and c are constants of the system, and

$$f(x) = a_o + a_1 x + a_2 x^2 + \ldots$$

Solutions of Eq. 1.1 predict subharmonic response under certain conditions. Stoker [2], Hayashi [3], and others have explored these solutions in some detail.

Recently, nonlinear wave interactions have been shown to produce subharmonic waves at ultrasonic frequencies in liquids. In 1965, Kuljis [4] observed subharmonic generation in water at around 300 kHz in a cavity, using two spherical bowl transducers to focus the sound. The cavitation threshold was very low, so that subharmonics were present only during the nonlinear cavitation process.

Cavitation and focusing, which immensely complicate an analytical analysis, are not required for subharmonic generation. Korpel and Adler [5], using an acoustic Fabry-Perot interferometer operating around 5 MHz in water, observed subharmonics at intensities well below the cavitation threshold. Analysis of the waveforms present in the cavity was accomplished by observation of the optical diffraction pattern produced by passing monochromatic light through the standing wave sound field. From Eq. A.4 in the Appendix, it can be seen that the spacing of diffraction orders is directly proportional to the sound frequency. Hence, the appearance of additional orders between the orders due to the fundamental wave was attributed to the presence of subharmonic waves in the cavity. If the cavity was driven at a multiple of the

TABLE 1.1

Terminology for various frequencies of the system.

SYMBOL	TERM	EXPLANATION
f	fundamental (or pump) frequency	The frequency used to excite the cavity.
f_o	fundamental cavity resonant frequency	The lowest frequency at which a standing wave can exist in the cavity, i.e. the effective cavity length is equal to $\lambda_o/2$, where λ_o is the wavelength of a wave of frequency f_o in the fluid.
f_s	subharmonic frequency	Frequencies in the cavity lower than f, due to nonlinear coupling to the pump frequency.
f_{tr}	transducer resonant frequency	Resonant frequency of transducer which is driven at the pump frequency.

fundamental cavity resonant frequency (see Table 1.1), they observed subharmonics above a certain energy density threshold in the water. The subharmonics occurred in pairs such that the sum of the two frequencies was always equal to the pump frequency. Also, the subharmonics were observed to be multiples of f_o, and consequently are at resonance in the cavity. The subharmonic frequencies were all in the vicinity of f/2. In 1966, McCluney [6] and Breazeale [7], utilizing the optical diffraction pattern and electronic means to determine the subharmonic frequencies, concluded that subharmonics occur at integral sub-multiples of the pump frequency. Since a given subharmonic could be obtained at several successive cavity resonances, the subharmonic is very seldom at resonance in the cavity, a result incompatible with the results of Korpel and Adler.

Several questions arise from these two studies. Are the subharmonics at a cavity resonance or not? What are the acoustic pressures of the fundamental and subharmonics at threshold? What factors influence the thresholds for the various subharmonics? How does the type of reflector and its thickness effect subharmonic generation? In this study, initiated late in 1965, subharmonic generation in an acoustic Fabry-Perot cavity is systematically investigated, in an attempt to answer these and other questions.

CHAPTER II

APPARATUS

The acoustic Fabry-Perot interferometer is composed of two air-backed, x-cut quartz transducers, submerged in water, and accurately aligned such that the front surfaces are parallel. Each transducer assembly is mounted on an optical bench, which allows the separation between them to be varied from 0.5 cm. to 30 cm. Each transducer may be easily replaced with other transducers of varying thickness. Two spring loaded adjustment screws, pivot the reflecting surfaces about two perpendicular axes in the plane of the transducer faces to within 0.05 degree.

A stable, variable frequency transmitter with a maximum output power of 100 watts excites one transducer, whose resonant frequency in water is 2975 kHz. The other transducer serves as a reflector and as a receiver for electronic analysis of waveforms present in the cavity.

Both optical and electronic techniques are used to study the waveforms present in the cavity. Electronic analysis is accomplished with a Singer Metrics SB 12 spectrum analyser connected to the quartz reflector, as in Fig. 2.1. The analyser displays amplitude as a function of frequency, causing a sinusoidal signal to appear as a vertical "pip" of height proportional to its amplitude. In order to compensate for the non-uniform response of the quartz to various frequencies, the response curves as a function of frequency of each quartz transducer to be used as a reflector, was ascertained. A frequency counter measures the transmitter frequency directly; the frequencies of

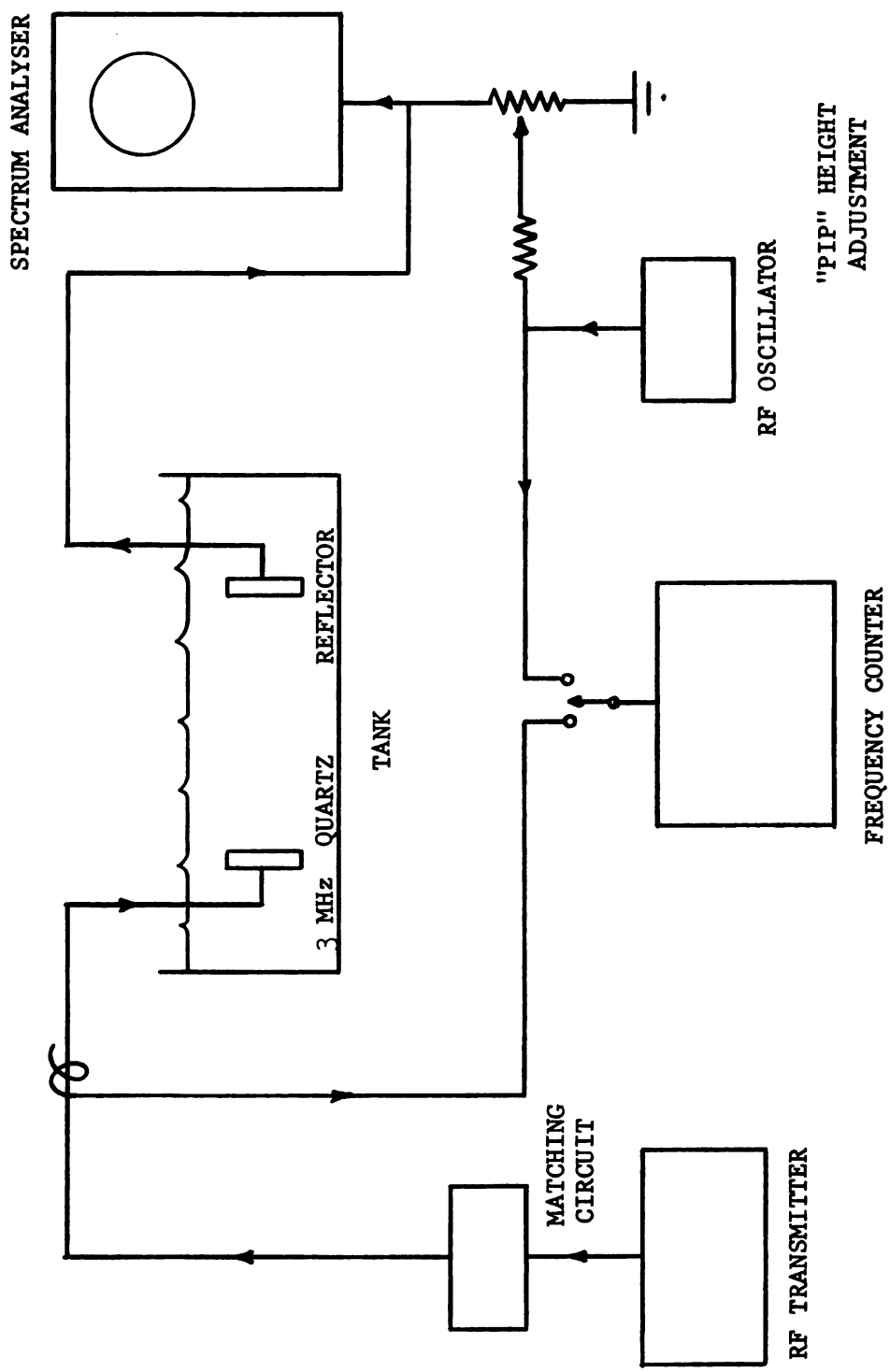

Figure 2.1 . Experimental arrangement of electronic equipment.

the subharmonics seen on the analyser screen may be measured by superimposing a "pip" from a low power oscillator, on top of the subharmonic "pip" on the analyser screen. Then the counter measures the frequency of the oscillator. If care is used when superimposing the two "pips", it is possible to measure the subharmonic frequencies to better than 500 Hz.

The transmitter used to excite the quartz transducer which drives the cavity has the facility for frequency adjustment to about one Hz at 3 MHz, and has a short term stability of better than one Hz at 3 MHz.

The optical system is shown in Fig. 2.2. A helium-neon gas laser with 1.0 milliwatt output power, in conjunction with a beam expander, provides a 5 cm diameter beam of parallel light. The entire interferometer assembly is oriented so that the standing wave sound field in the cavity is perpendicular to a beam of parallel monochromatic light. Stop S_1 allows only that light which passes through a uniform portion of the sound field to pass on to lens L_1. A single lens reflex camera, with its ground glass screen removed, is positioned at the focal point of lens L_1. The image formed at the camera location is magnified and projected onto a large screen by the prism and lens L_2.

The standing wave sound field in the cavity produces periodic changes in the index of refraction in the liquid, which causes a periodic retardation in the phase of the light as it passes through the liquid, and results in a diffraction pattern at the camera location and on the screen. The detailed structure of the diffraction pattern can be observed on the screen and then recorded on film immediately by actuating

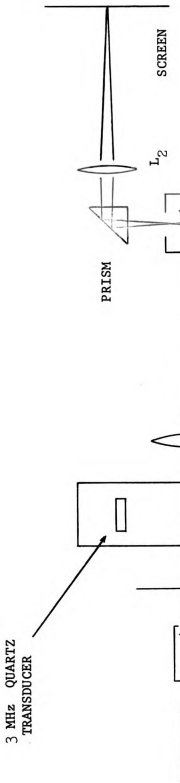

Figure 2.2 . Experimental arrangement of optical equipment.

the shutter mechanism. High magnification, necessary for visual observation, and good resolution on the film are easily obtained. The camera can be replaced with a photomultiplier, to measure relative intensities of the orders in the diffraction pattern when needed.

CHAPTER III

PROCEDURE

To align the interferometer system, two alignment criteria must be satisfied: 1) the two transducers must be parallel to each other, and 2) the light beam must be perpendicular to the sound field between the transducers. The first requirement may be accomplished electronically by observing the rate of decay of a pulsed signal introduced into the cavity. As is shown in Fig. 3.1, the impedance of an Arenberg PG 650 pulsed oscillator is matched to the 2975 kHz quartz transducer, and the transducer is driven at its resonant frequency. An oscilloscope protrays the transmitted and reflected pulses, and the alignment screws are adjusted for an exponential decay envelope with a maximum in the number of visible reflected pulses. This method produces 30 or more reflected pulses and is a sensitive indication of correct alignment within the stated accuracy of 0.05 degree.

The second requirement is obtained next, by removing the reflector assembly to allow a progressive wave to interact with the light beam. From Raman and Nath [8] theory, the diffraction pattern from a progressive wave will be symmetric around the zeroth order, only if the light and sound are perpendicular. This adjustment is made visually. After replacing the reflector assembly, the first procedure is repeated to guarantee parallelism. The pulse alignment is repeated whenever either transducer assembly is moved along the optical bench assembly, or removed from it for any reason.

The interferometer cavity is brought into resonance by

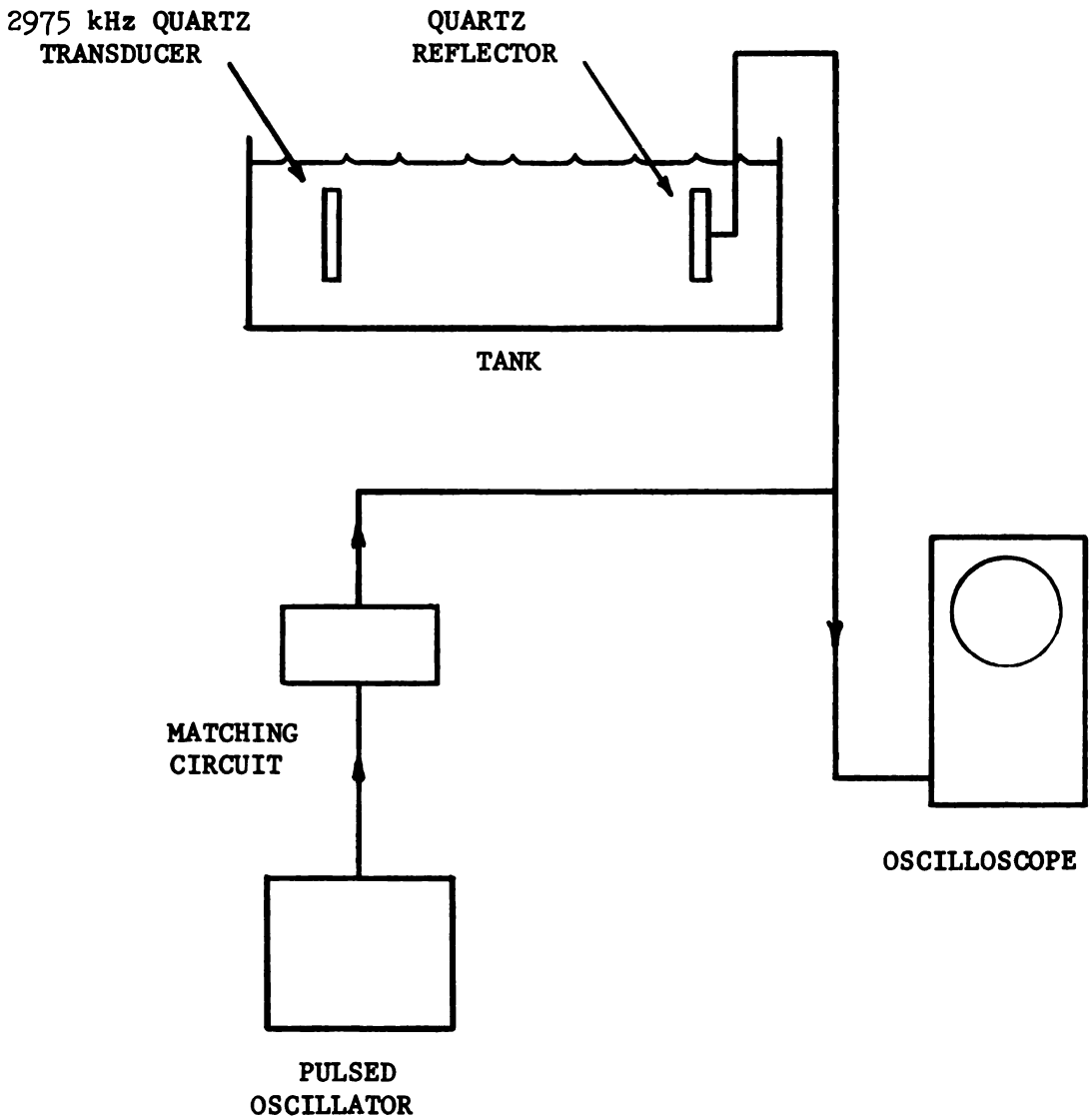

Figure 3.1 . Electronic pulse alignment arrangement.

adjustment of the transmitter frequency for a maximum in the sound intensity in the cavity, which occurs when there is a maximum in the number of orders in the diffraction pattern. The frequency change between adjacent maxima is a measure of f_o, the fundamental cavity resonant frequency (see Table 1.1).

When searching for subharmonic generation, the characteristic splitting of the diffraction pattern is used as the primary indication of the existence of subharmonics. Detailed analysis can then be made electronically. Spurious responses in the spectrum analyser can be identified by their continued existence, when the subharmonics are extinguished by slightly altering the transmitter frequency.

The frequencies and thresholds of all attainable subharmonics were measured for various cavity configurations. A systematic study of the effects of reflector type and thickness, fundamental frequency, and separation of transducers was conducted. The acoustical pressures of the fundamental and subharmonic waves at threshold were measured for several cavity configurations using optical methods.

CHAPTER IV

RESULTS

Analysis of the waveforms present in the interferometer with the spectrum analyser indicates that whenever the optical diffraction pattern splits, there are always new frequencies occurring in pairs, such that

$$f_s^{(1)} + f_s^{(2)} = f \tag{4.1}$$

where $f_s^{(1)}$ and $f_s^{(2)}$ are the frequencies of the pair, and f is the fundamental frequency. Usually a single pair appears, but occassionally several pairs appear simultaneously. In every case, each subharmonic frequency always obeys the relation

$$f_s = n f_o \tag{4.2}$$

where f_o is the fundamental cavity resonant frequency, and n is an integer. These results agree completely with Korpel and Adler. Since the interferometer is also at resonance for the fundamental frequency f, the relation

$$f = m f_o \tag{4.3}$$

holds, where m is also an integer. Combining Eqs. 4.2 and 4.3, we obtain the condition

$$f_s = (n/m) f \tag{4.4}$$

The accuracy of Eq. 4.4 will be discussed later. Table 4.1 shows a small sample of data, illustrating Eq. 4.1 and 4.4.

Below a certain energy density of the fundamental frequency,

TABLE 4.1

Typical subharmonic data sample

f_o = 15.04 kHz

Reflector: 1.0 MHz quartz

Cavity length: 5.0 cm

Fundamental Frequency (kHz)	m	Subharmonic Frequency Pairs (kHz)	n
3115.9	207	1069.0	71
		2047.3	136
3130.3	208	1069.3	71
		2061.2	137
		1084.1	72
		2046.4	136
3145.2	209	1083.7	72
		2061.4	137
		1099.3	73
		2045.7	136

a given subharmonic will not appear. Slightly above this threshold, the subharmonic signal amplitude is relatively constant. The threshold level for each subharmonic depends on several factors, including accuracy of alignment of the interferometer itself. A representative curve is given in Fig. 4.1.

Not all frequencies satisfying cavity resonance produce subharmonics, so the frequency dependence was investigated. All subharmonics with attainable thresholds were measured over a fundamental frequency range covering 2.4 MHz to 3.6 MHz. A quartz transducer with a thickness corresponding to a 2.0 MHz resonance was used as a reflector, and the separation distance was 5.0 cm. Figure 4.2 shows the result in terms of the integers m and n defined in Eqs. 4.2 and 4.3, with each subharmonic plotted as a dot. The symmetry around a line through

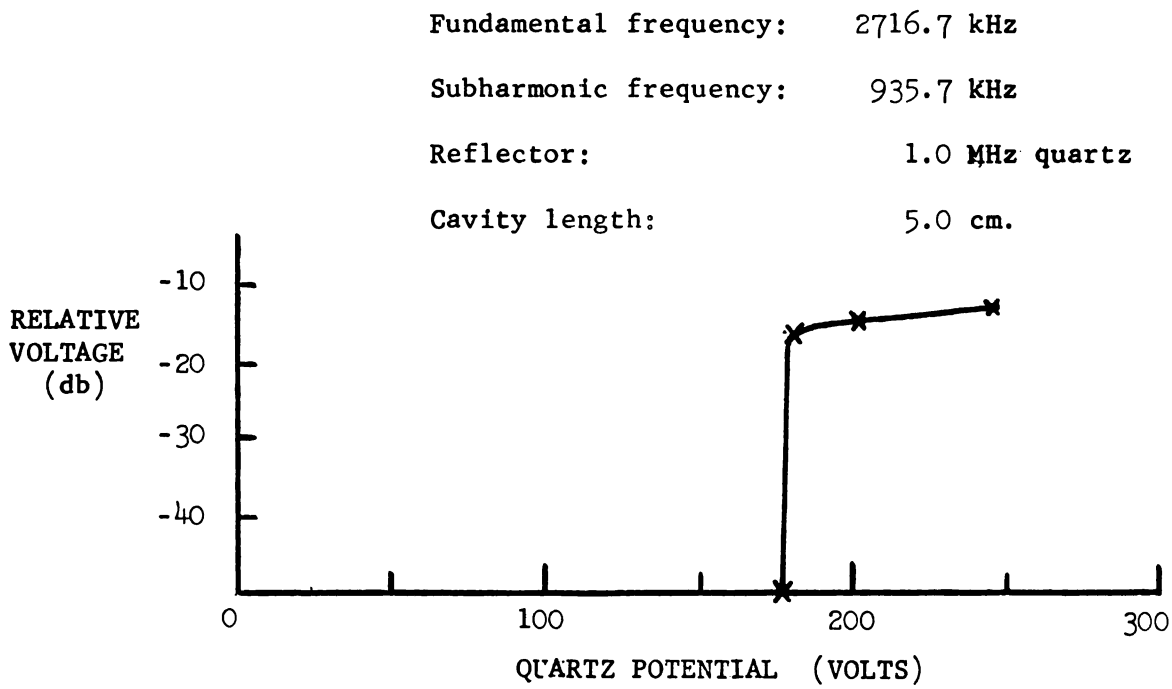

Figure 4.1 . A typical subharmonic threshold curve.

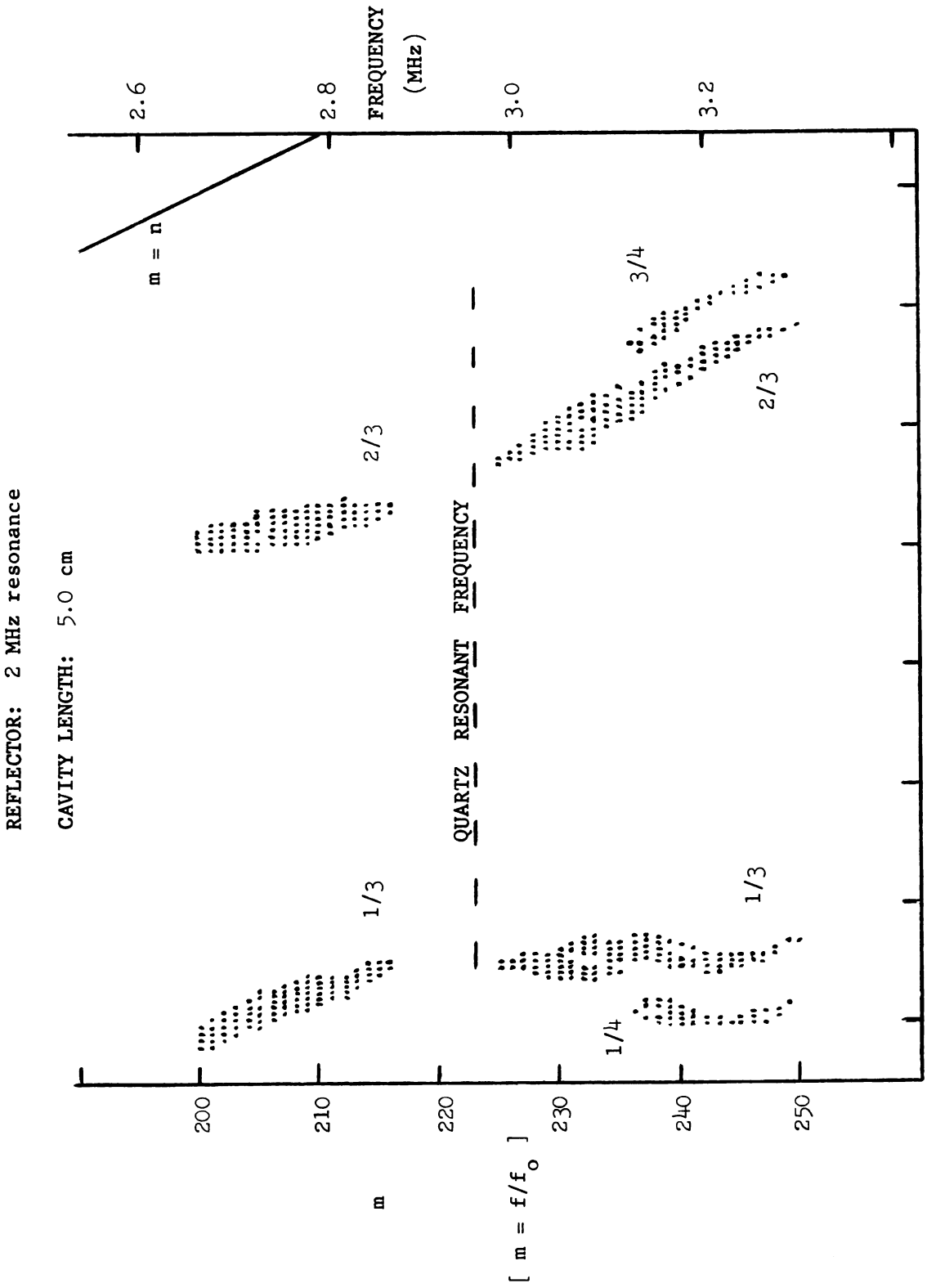

Figure 4.2 . Graph of observed subharmonics.

n = m/2 illustrates Eq. 4.1. Two items of importance should be pointed out. First, there is a gap around the resonant frequency of the driven quartz within which no subharmonics occur. Second, all of the lower frequency subharmonics of each pair are within a few percent of 1/3 or 1/4 of the pump frequency.

The thresholds of each subharmonic, measured in terms of the potential across the driven transducer, are shown in Fig. 4.3. Each curve in the figure is a cross section of Fig. 4.2 for a fixed value of n. Only a few cross sections for n values in the neighborhood of 60 to 80 are plotted. The cross sections for n values from 140 to 180 will yield redundant threshold information, since all subharmonics occur in pairs, but the shapes of the individual curves will be quite different, of course.

Figures 4.4 and 4.5 show the results of changing the reflector, everything else held constant. A quartz with a 1.0 MHz resonance was used at a distance of 5.0 cm from the driven quartz. Again the lack of subharmonics around the resonant frequency of the driven quartz is evident. However, the presence of subharmonics around f/2 is new. Also, the subharmonics are spread over a much larger frequency band and frequencies around f/4 are absent.

With subharmonics near f/2, and even m, a single subharmonic of frequency f/2 appears most frequently, although a pair of subharmonics, both near f/2, occasionally appear. It m is odd, often several pairs appear simultaneously, all with the same threshold. Every subharmonic with a frequency near f/2 is present, as in Fig. 4.6.

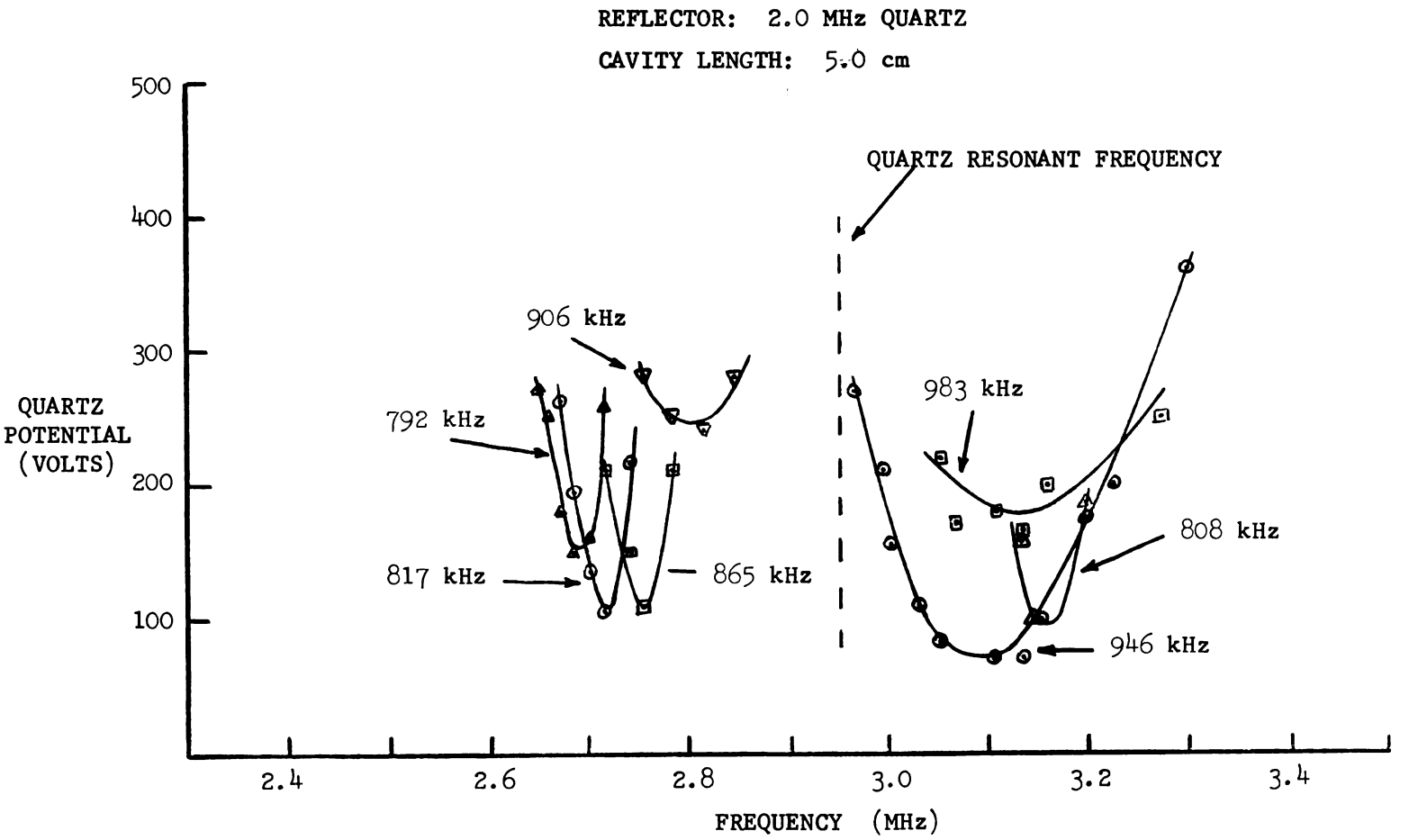

Figure 4.3 . Graph of subharmonic thresholds.

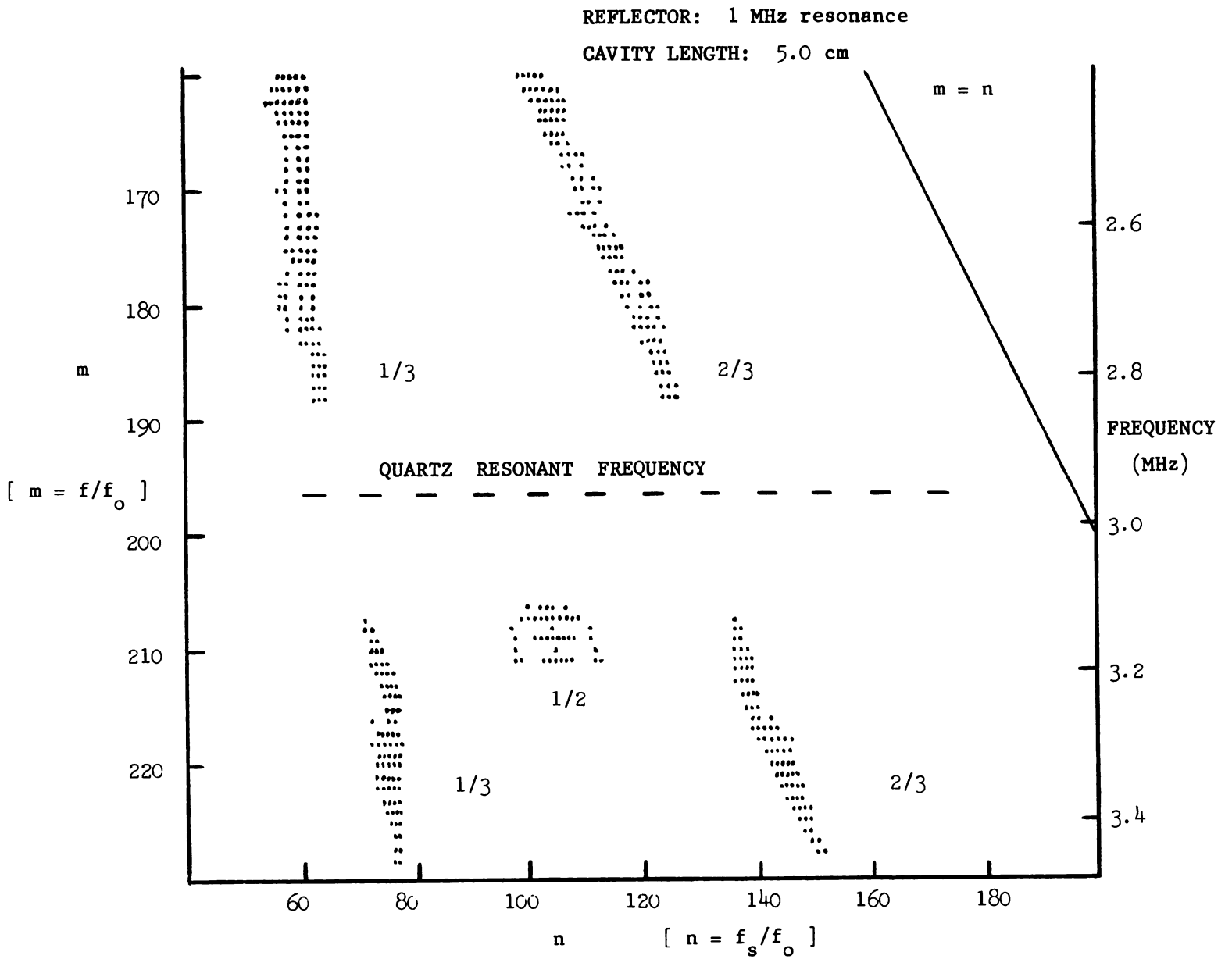

Figure 4.4 . Graph of observed subharmonics.

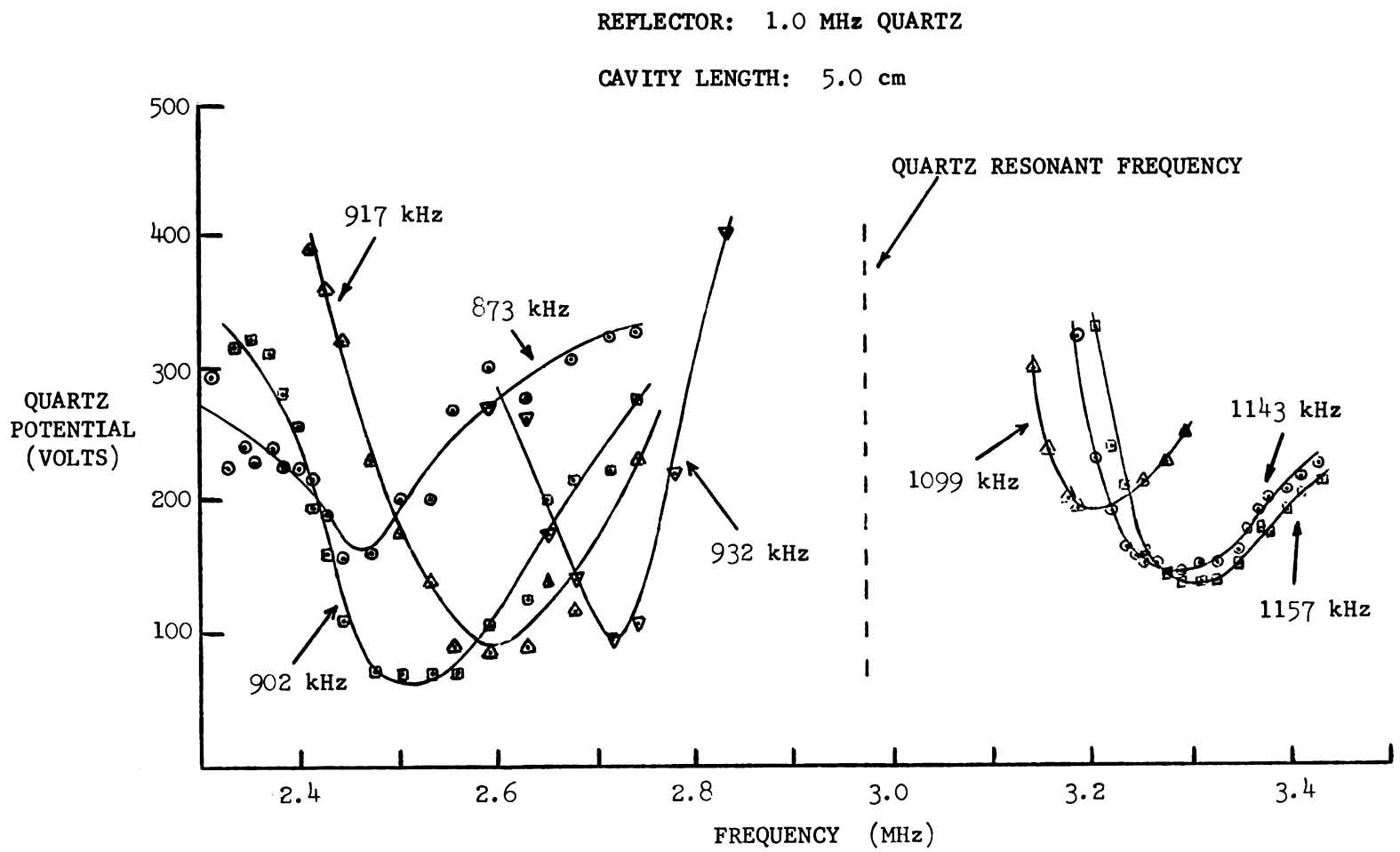

Figure 4.3 . Graph of subharmonic thresholds.

Other quartz reflectors were examined in less detail. Thicknesses corresponding to resonant frequencies of 1.2 MHz, 1.5 MHz, 3.0 MHz, 3.5 MHz and 4.0 MHz were used. All exhibit the phenomenon of no subharmonics around the resonant frequency of the driven quartz. Results similar to the preceding examples were obtained. although thresholds were very high for the 3.0 MHz reflector and subharmonics only occurred in a narrow frequency region just above 3 MHz. Figure 4.7 summarizes this survey, showing all regions where subharmonics were obtained in terms of the driving frequency. These "bands" appear to lie in regions around 1/2, 1/3, and 1/4 of the pump

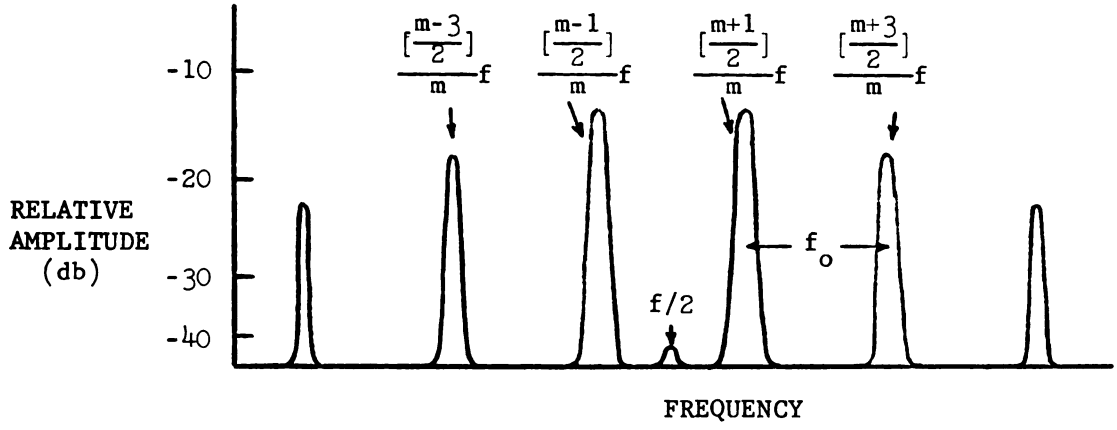

Figure 4.6 . Spectrum analyser tracing of subharmonics around f/2 for the case where m is odd.

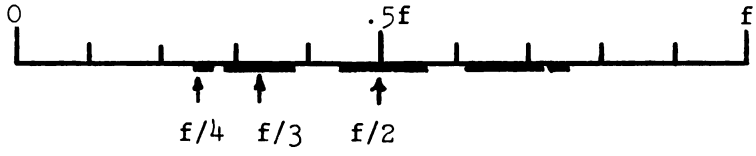

Figure 4.7 . Bands of observed subharmonic frequencies in terms of the driving frequency f.

frequency, although a more extensive survey might indicate otherwise.

Investigations into the range of cavity lengths for which subharmonics will occur reveals that at small distances (2 cm and less), it becomes more difficult to produce subharmonics, as the thresholds become very high. The same thing happens with distances of 8 to 10 cm and more. For any particular reflector, the curve will be different, but in general, 4 to 6 cm produced minimum thresholds, everything else held constant. Hence, most work was done around this region.

All of the air-backed quartz reflectors introduce a frequency dependent phase shift upon a wave during reflection. A reflector with a constant phase shift was constructed in an attempt to determine what effect phase changes have on the system. A brass cylinder was constructed with saw cuts angled into the rear surface to scatter any sound reaching it, as in Fig. 4.8. Treating the reflection as a single boundary infinite medium problem, the ratio of reflected to incident sound intensity is 0.847. The angle of the cuts is determined to minimize reflections [9]. A search was conducted at

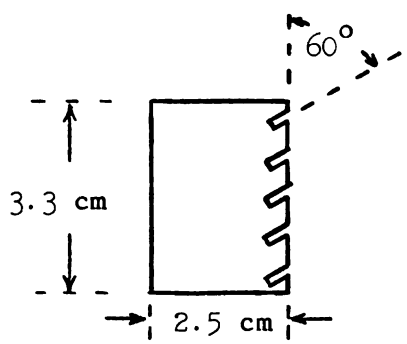

Figure 4.8 . Brass reflector.

frequencies from 2.5 MHz to 3.5 MHz and with cavity lengths of 3.0 cm to 9.0 cm. No subharmonics were obtained under any circumstances, even with a potential of 600 volts or more across the driven quartz transducer.

The subharmonics are extremely sensitive to small changes in frequency around the resonance of the interferometer. Changes of less than 10 Hz in the driving frequency will extinguish a subharmonic for an energy density slightly above threshold. Considerably above threshold level, changes of 5 to 10 Hz will often "coax" the system to jump to an adjacent mode, i.e. the subharmonic n/m will extinguish and be replaced by another, say (n + 1)/m. Occasionally, when well above threshold, two or three subharmonics with nearly the same frequency may exist simultaneously (each has a corresponding subharmonic obeying Eq. 4.1, of course). In Fig. 4.9, a typical cavity resonance illustrates the presence of subharmonics around f/4 and f/3, somewhat above the minimum thresholds.

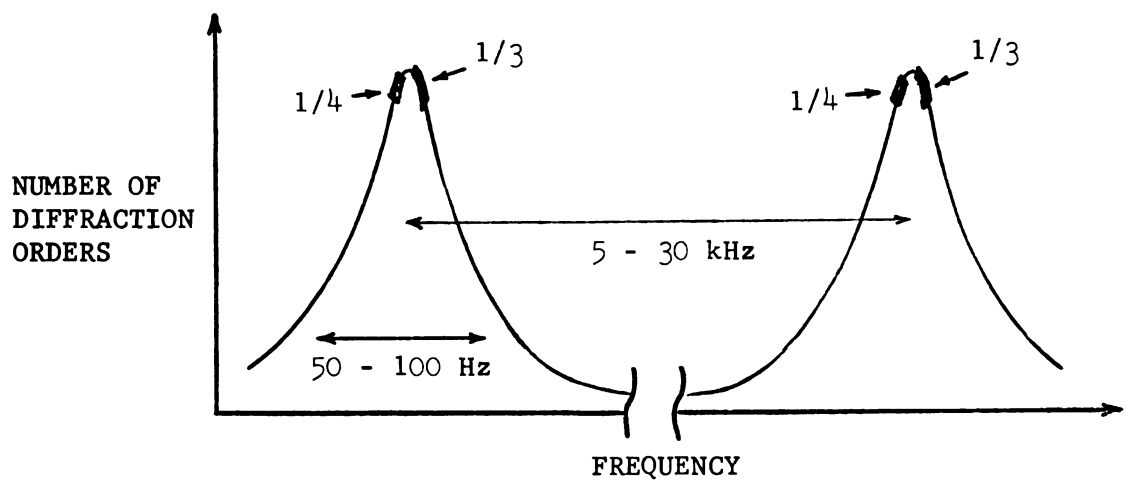

Figure 4.9 . Typical cavity resonance, showing regions for which subharmonics occur.

Heating effects in the cavity often interfere with subharmonic generation; drifting of the cavity length will necessitate continual corrections to be made in the fundamental frequency if subharmonics are to be maintained. This problem is more pronounced under experimental conditions where thresholds are high. Hence, most work was done using conditions where subharmonic thresholds are moderate.

Previously, it was stated that parallelism of the transducers comprising the interferometer is confined to about 0.05 degree. To this accuracy, checks were made of the effect of misalignment on the system. Gross misalignment, of the order of 0.5 degree, is enough to extinguish all subharmonics under any conditions. However, within the range of 0.5 and 0.05 degree the only significant change observed is to raise the threshold curves upward in Fig. 4.3 and Fig. 4.5. The general features remain about the same. This characteristic gives a double check on the pulse method of alignment.

The relative sound pressure in the cavity as a function of frequency, due to the fundamental frequency standing wave, was measured optically, using a photomultiplier to measure the intensity of the zeroth order in the diffraction pattern (see Appendix). Figure 4.10 shows the result for a 1.0 MHz quartz reflector and a cavity length of 5.0 cm. The curve is essentially discrete, since very little sound pressure is produced unless the cavity is excited at a multiple of f_o. Also, the energy density of the fundamental wave is well below the subharmonic threshold level. A response curve for the driven quartz transducer (taken under progressive wave conditions) is superimposed on the same figure for comparison purposes later.

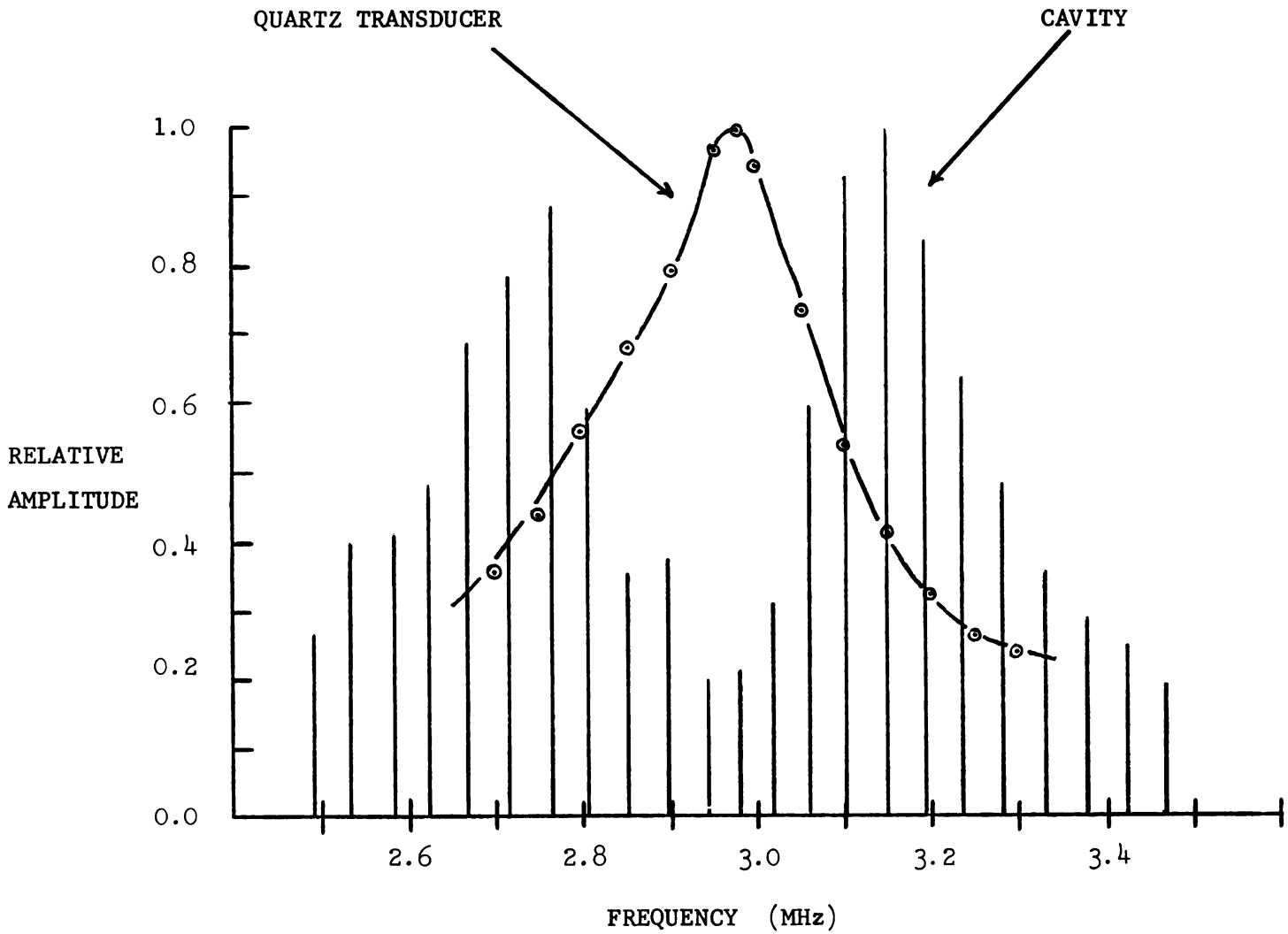

Figure 4.10 . Response curves for quartz transducer and cavity, showing relative sound pressure.

The magnitudes of the fundamental and subharmonic pressures in the cavity at the threshold energy density were determined by a combined optical-electronic method. The fundamental pressure is determined optically by measuring the light intensity of the zeroth order in the diffraction pattern on the low side of threshold. The subharmonic pressure is measured on the spectrum analyser just above threshold, after calibration of the analyser by a similar optical technique. Assuming the subharmonic depletes a negligible amount of energy from the fundamental wave, a pressure comparison can be made.

Under typical conditions, the peak pressure of the fundamental wave at threshold is around 1.5 atmosphere, corresponding to a peak density variation of $\Delta\rho/\rho = 6.4 \times 10^{-5}$. The subharmonic pressures are typically about one tenth of the fundamental pressure; the assumption is therefore valid, since the energy is only 10^{-2} times that of the fundamental wave.

In Fig. 4.11, several photographs display diffraction patterns resulting from the presence of subharmonics in the cavity. The first three illustrate subharmonic generation at frequencies near 1/2, 1/3, and 1/4 of the pump frequency; in the fourth photograph, the subharmonics deviate sufficiently from integral submultiples of the pump frequency, so that the detailed substructure is visible.

Equation A.16 predicts multiple diffraction. That is, each diffraction order due to one wave will, in turn, be re-diffracted by the other waves. That this is indeed the case, can be seen in Fig. 4.11, where diffraction orders of the fundamental and the lower

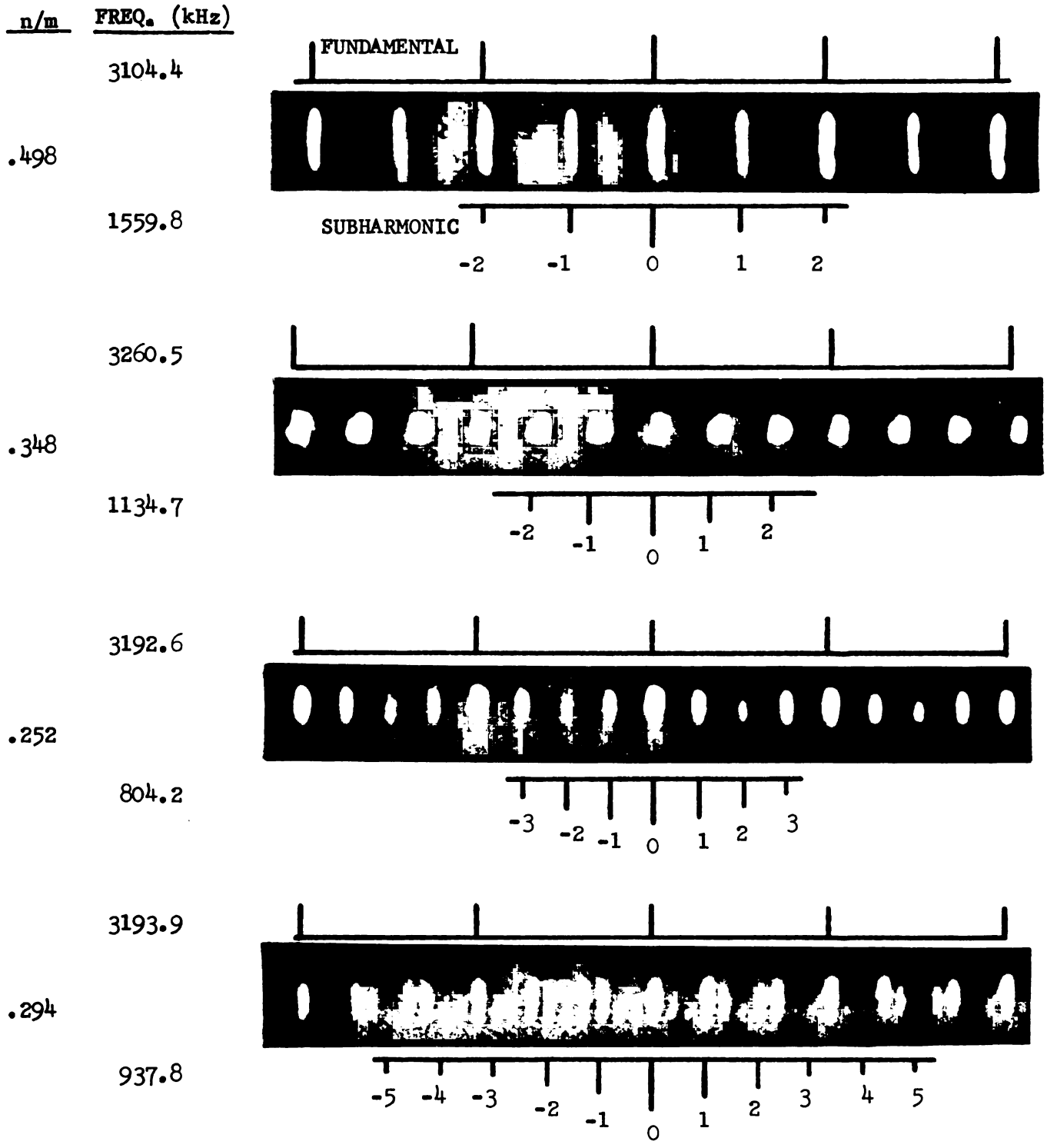

Figure 4.11 . Diffraction pattern photographs obtained during subharmonic generation.

frequency subharmonic wave are marked above and below each photograph, respectively. Only the subharmonic orders diffracted from one fundamental order are marked to avoid confusion in the figure. The photographs also illustrate that the intensities of the subharmonic orders are nearly equal to the fundamental intensities. This is to be expected, even though the subharmonic pressures are only one-tenth of the fundamental pressure, since both pressure values are large enough to lie on the relatively flat portions of the curves in Fig. A.1.

CHAPTER V

DISCUSSION

At the present time, a theory to explain the experimental observations made in this study is not available. Difficulties arise when attempts are made to solve the equations of motion for a fluid [10] with standing waves, unless the inherent nonlinearity is neglected. However, a qualitative understanding of a few aspects of the system may be obtained.

A standing wave in an acoustic interferometer is subject to several loss mechanisms, including absorption of the wave by the liquid, spreading of the sound field, and nonlinear effects which couple energy into other frequencies. These losses are just cancelled out for the fundamental frequency wave by the energy supplied by the quartz transducer at one end of the cavity. However, for a subharmonic wave in this cavity, the loss can only be made up by a coupling of energy at other frequencies into the subharmonic frequency by some nonlinear mechanism. Since all energy initially came from the fundamental frequency, there will be a certain level of energy at the fundamental frequency for which the loss at the subharmonic frequency is just cancelled. Above this energy level, the subharmonic wave will grow to an intensity for which the gain-loss balance is regained. Hence, a threshold curve similar to Fig. 4.1 is expected. Also, unless the subharmonic wave obeys Eq. 4.2, it will not be at a cavity resonance frequency, causing additional losses and raising the threshold to a very high energy level.

High thresholds at large separation distances are most likely due to the appreciable beam spread and consequent loss of energy in the system. Absorption losses in water are small, being around

0.02 db/cm, and therefore will not contribute significantly. At small distances, high thresholds may be due to less coupling between the two waves because of the small distances involved, although the losses should also become much smaller. The "near field" of the transducer may also influence the thresholds, due to the inhomogeneity in the sound field near the transducers. In any case, the liquid appears to be the nonlinear mechanism, rather than the transducers, or the transducer-liquid interface, although more evidence certainly is needed.

The relative phase changes of fundamental and subharmonic waves upon reflection appear to strongly influence which n/m ratios are permitted to exist in the cavity and in what their thresholds will be. The brass reflector may be treated as a single boundary problem, since the rear surface will scatter most of the sound reaching it. The ratio of reflected to incident amplitude, denoted the reflection coefficient, is

$$R = \frac{1 - \frac{\rho_2 v_2}{\rho_1 v_1}}{1 + \frac{\rho_2 v_2}{\rho_1 v_1}} \qquad (5.1)$$

where ρ_1 and v_1 are the density and sound velocity respectively in the incident material, and ρ_2 and v_2 refer to the same quantities in the reflecting material. Similarly, a water-quartz-air combination, treated as a two boundary problem with the ρc of air assumed to be negligibly small, yields the complex reflection coefficient

$$R(k) = \exp\left[-2i \tan^{-1}\left(\frac{\rho_2 c_2}{\rho_1 c_1} \tan k d\right)\right] \qquad (5.2)$$

where the subscripts 1 and 2 refer to water and quartz, respectively, k is the wave constant for longitudinal waves in the x-direction in quartz, and d is the quartz thickness. It is important to note that Eq. 5.2 exhibits a frequency dependent phase shift, whereas Eq. 5.1 does not. The complete absence of subharmonic generation using a brass reflector seems to indicate that a frequency dependent phase shift is a requirement for subharmonic generation. Additional evidence is provided by Fig. 4.9, where we see that slight frequency deviations from cavity resonance may allow a subharmonic to exist by satisfying certain phase requirements, even though the fundamental frequency is not quite in resonance in the cavity.

The above discussion implies that Eq. 4.4 does not hold strictly, since m and n are not exactly integers. However, the deviation in m is very small, as can be seen from Fig. 4.9, being less than one part in 100. The frequency measurements leading to Eq. 4.2 indicate that n is an integer to about one part in 10, which will completely mask the deviations in m, so Eq. 4.4 is correct to within about one part in 10.

The dip in the center of the cavity response curve in Fig. 4.10 is a common feature in coupled oscillator problems in many fields. The lack of subharmonics around the driven quartz transducer's resonant frequency is at least partially due to this phenomenon. Due to the low sound intensity in this region, even for high potential across the

driven quartz transducer, it was not possible to reach an energy density sufficient to produce subharmonics. However, the possibility of a feature inherent in the system which prevents subharmonic generation at the resonant frequency of the driven quartz should not be eliminated.

APPENDIX

Ultrasonic Light Diffraction Theory

The diffraction of light by ultrasonic waves is a convenient method of determining much about the ultrasonic wave and the medium through which it travels. Analysis of the diffraction pattern produced by the sound field in an acoustic Fabry-Perot interferometer yields information about the frequencies and pressures of the various waves that are present.

The sound field produces periodic changes in the index of refraction of the medium around its undisturbed value when the sound is not present. A plane wave of light, impinging upon this disturbance, will be in some way altered. For moderate frequencies, sound intensity, and path length of the light through the sound beam, the light will be modulated in phase with a periodicity of the sound field when it emerges on the other side of the sound beam. The phase modulated light can be resolved into a series of plane waves, each traveling in a slightly different direction, which will form a diffraction pattern if focused on a screen.

From the diffraction integral, it is known that the amplitude distribution of the diffracted light due to a phase grating is given by

$$A(\theta) = C\, e^{i\omega t} \int_{-D}^{D} \exp \left\{ i \left[\frac{2\pi x}{\lambda} \sin \theta + v(x,t) \right] \right\} dx, \qquad (A.1)$$

where θ is the angle of deviation of the light, ω is the angular frequency of the light, λ is the wavelength of the light, 2D is

the width of the light beam, and C is a normalization constant. The parameter $v(x,t)$ is a dimensionless parameter describing the change of the index of refraction, and is related to the acoustical pressure $p(x,t)$ by

$$v(x,t) = \frac{2\pi L \kappa}{\lambda} \quad p(x,t) \quad , \quad (A.2)$$

where L is the width of the sound beam, and κ is the piezo-optic coefficient of the medium.

For a single stationary wave in the cavity, the acoustical pressure may be written as

$$p(x,t) = p_o \left[\sin(\omega^* t - k^* x) + \sin(\omega^* t + k^* x)\right] \quad , \quad (A.3)$$

where ω^* is the angular frequency of the sound, and k^* is the wave constant of the sound.

Solving Eq. A.1, leads to a discrete light distribution with light occurring only at angles

$$\sin \theta_n = \frac{n \lambda}{\lambda^*} \quad , \quad (A.4)$$

where n is an integer. The time averaged light intensities are given by

$$\overline{I_n} = \sum_{r=-\infty}^{+\infty} J_r^2 (v_o) \, J_{r-n}^2 (v_o) \quad , \quad (A.5)$$

where J_r is the r^{th} order Bessel Function, and $v_o = \frac{2\pi L \kappa}{\lambda} p_o$.

Equation A.4 is more general than the above indicates, and holds for any periodic sound field provided the light impinges normally.

Figure A.1 shows how the first few diffraction orders vary in intensity with pressure [11]. Note that if $\overline{I}_n$ is measured experimentally, and the piezo-optic coefficient is known, the acoustic pressure may be determined.

When subharmonics are present, Eq. A.3 must be generalized. For the common case of only two subharmonics with

$$f_s^{(1)} + f_s^{(2)} = f \quad ,$$

we may write

$$p(x,t) = \sum_{j=0}^{2} p_j[\sin(\omega_j^* + - k_j^* x) + \sin(\omega_j^* t + k_j^* x)], \quad (A.6)$$

where the subscripts 0, 1, and 2 refer to the fundamental, subharmonic $f_s^{(1)}$, and subharmonic $f_s^{(2)}$, respectively. Combining Eqs. A.6 and A.2, results in

$$v(x,t) = \sum_{j=0}^{2} v_j [\sin \alpha_j + \sin \beta_j] \quad (A.7)$$

where

$$v_j = \frac{2\pi L \kappa}{\lambda} p_j \quad ,$$

$$\alpha_j = \omega_j^* t - k_j^* x \quad ,$$

and

$$\beta_j = \omega_j^* t + k_j^* x \quad .$$

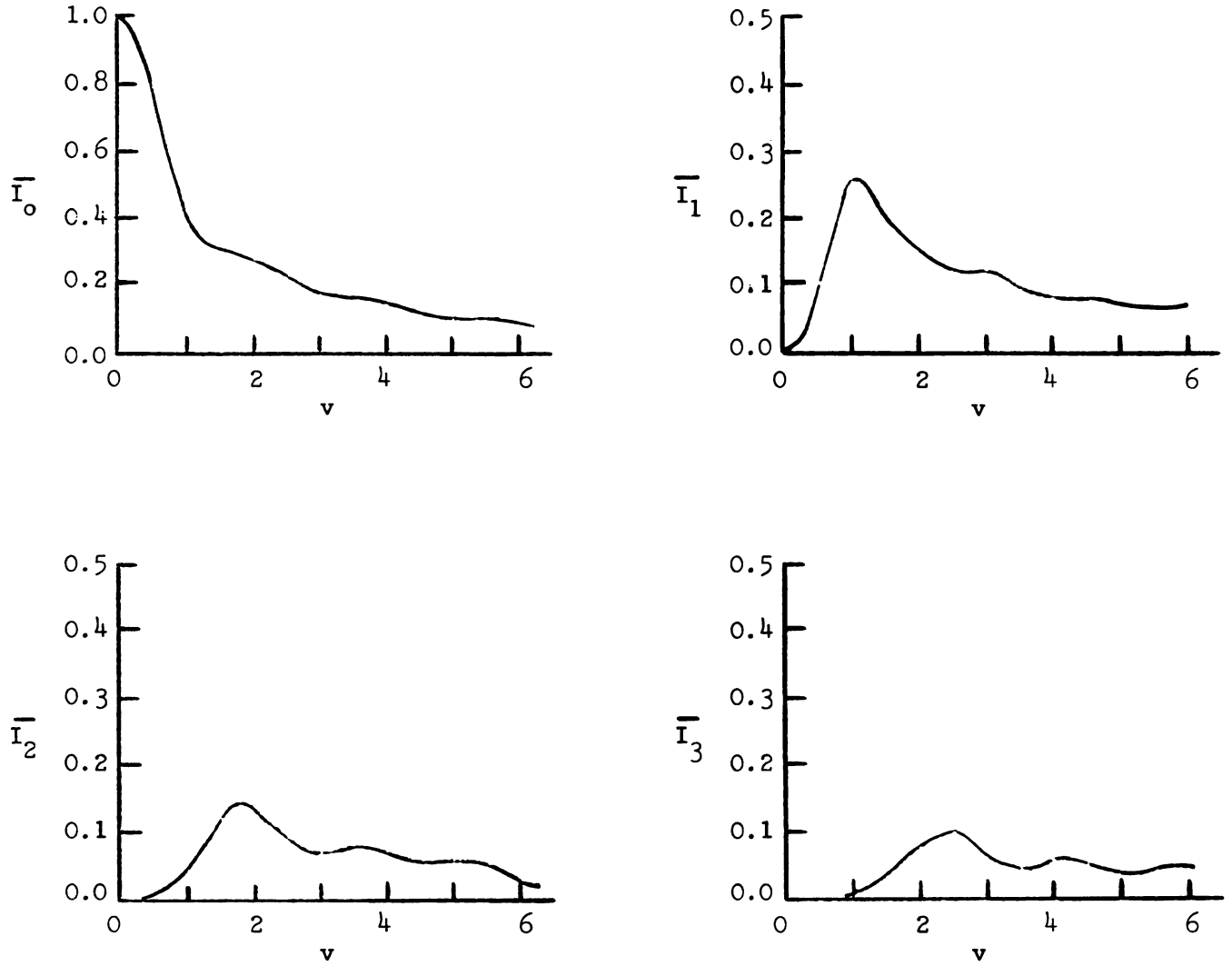

Figure A.1 . Graph of average light intensities in the first few diffraction orders, for a stationary wave.

Using the identity

$$\exp [i\ a \sin \phi] = \sum_{r=-\infty}^{+\infty} J_r (a) \exp[i\ r\ \phi], \qquad (A.8)$$

where J_r is the r^{th} order Bessel Function, and inserting Eq. A.7 into Eq. A.1, we obtain

$$A(\theta) = C\ e^{i\omega t} \sum_{\substack{m,n,q \\ =-\infty}}^{+\infty} \sum_{\substack{r,s,u \\ =-\infty}}^{+\infty} J_m(v_o)\ J_n(v_o)\ J_q(v_1)\ J_r(v_1)\ J_s(v_2)\ J_u(v_2)$$

$$\times \int_{-D/2}^{D/2} \exp\left[i\left(\frac{2\pi x}{\lambda} \sin\theta + m\alpha_o + n\beta_o + q\alpha_1 + r\beta_1 + s\alpha_2 + u\beta_2\right)\right] dx\ . \qquad (A.9)$$

Evaluating the integral in Eq. A.9, we obtain

$$A(\theta) = C\ e^{i\omega t} \sum_{\substack{m,n,q \\ =-\infty}}^{+\infty} \sum_{\substack{r,s,u \\ =-\infty}}^{+\infty} J_m(v_o)\ J_n(v_o)\ J_q(v_1)\ J_r(v_1)\ J_s(v_2)\ J_u(v_2)$$

$$\times \frac{2 \sin\left\{\left[\frac{2\pi}{\lambda} \sin\theta + k_o^* (n-m) + k_1^* (r-q) + k_2^* (u-s)\right] D\right\}}{\frac{2\pi}{\lambda} \sin\theta + k_o^* (n-m) + k_1^* (r-q) + k_2^* (u-s)}$$

$$\times \exp\left\{it\left[\omega_o^* (m+n) + \omega_1^* (q+r) + \omega_2^* (s+u)\right]\right\} \qquad . \quad (A.10)$$

With no sound present, $v_o = v_1 = v_2 = 0$, and $A(\theta) = \delta(\theta)$. Using this to evaluate the normalization constant, we obtain

$$c = \frac{1}{2D} \quad . \tag{A.11}$$

If the quantities $j = m - n$, $k = q - r$, $\ell = s - u$, and

$$W_{jk\ell} = \frac{\sin\left[\left(\frac{2\pi}{\lambda}\sin\theta - j\,k_o^* - k\,k_1^* - \ell\,k_2^*\right) D\right]}{\left[\frac{2\pi}{\lambda}\sin\theta - j\,k_o^* - k\,k_1^* - \ell\,k_2^*\right] D}$$

are defined, Eq. A.10 reduces to

$$A(\theta) = \sum_{\substack{j,m,k,q,\\ \ell,s=-\infty}}^{+\infty} J_m(v_o)\, J_{m-j}(v_o) J_q(v_1)\, J_{q-k}(v_1)\, J_s(v_2)\, J_{s-\ell}(v_2)$$

$$\times W_{jk\ell}\, \exp\left\{ it[\omega + \omega_o^*(2m - j) + \omega_1^*(2q - k) + \omega_2^*(2s - \ell)]\right\} . \tag{A.12}$$

For the limiting case as D approaches infinity, $W_{jk\ell} \neq 0$ only if

$$\frac{2\pi}{\lambda}\sin\theta - jk_o^* - kk_1^* - \ell\,k_2^* = 0 \quad .$$

Rewriting Eq. A.13 as

$$\sin\theta = \frac{\lambda}{\lambda_o^*}\, j + \frac{\lambda}{\lambda_1^*}\, k + \frac{\lambda}{\lambda_2^*}\, \ell \quad ,$$

and using the fact that

$$\frac{1}{\lambda_o^*} = \frac{1}{\lambda_1^*} + \frac{1}{\lambda_2^*} \quad ,$$

finally gives the relation

$$\sin \theta_{j'k'} = \frac{\lambda}{\lambda_o^*} j' + \frac{\lambda}{\lambda_1^*} k' \quad , \qquad (A.14)$$

where $j' = j + \ell$ and $k' = k - \ell$. The amplitudes of the discrete orders are

$$A_{jk\ell} = \sum_{\substack{m,q,s \\ =-\infty}}^{+\infty} J_m(v_o)\, J_{m-j}(v_o)\, J_q(v_1)\, J_{q-k}(v_1)\, J_s(v_2)\, J_{s-\ell}(v_2)$$

$$\times \exp\left\{ it[\omega + \omega_o^* (2m - j) + \omega_1^* (2q-k) + \omega_2^* (2s - \ell)] \right\} \quad . \qquad (A.15)$$

The time averaged light intensities are

$$\overline{I_{jk\ell}} = \left[\sum_{m=-\infty}^{+\infty} J_m^2(v_o)\, J_{m-j}^2(v_o) \right] \left[\sum_{q=-\infty}^{+\infty} J_q^2(v_1)\, J_{q-k}^2(v_1) \right]$$

$$\times \left[\sum_{s=-\infty}^{+\infty} J_s^2(v_2)\, J_{s-\ell}^2(v_2) \right] \quad . \qquad (A.16)$$

Equations A.14 and A.16 describe the Fraunhofer diffraction pattern which results from the interference of light with a fundamental and two subharmonic standing waves which obey Eq. 4.1. Equation A.16 is true only under a phase grating assumption. This assumption is not entirely valid for the acoustical pressures observed in the

cavity. Therefore, intensities calculated with Eq. A.16 are only approximate. For a detailed discussion of the validity of the phase grating assumption, refer to Klein and Cook [12].

BIBLIOGRAPHY

[1] Lord Rayleigh, The Theory of Sound, Volume I, London, Macmillan and Co., 1877, pp.78-85.

[2] J. J. Stoker, Nonlinear Vibrations, Interscience Publishers, Inc., N. Y., 1950.

[3] C. Hayashi, Nonlinear Oscillations in Physical Systems, McGraw-Hill, N. Y., 1964.

[4] M. Kuljis, "Experimental Study of Acoustic Parametric Open Cavity Array-Amplifier", Electrotehnika, 1, 1965, pp.3-12.

[5] A. Korpel and R. Adler, "Parametric Phenomena Observed on Ultrasonic Waves in Water", Appl. Phys. Lett., 7, 15 August 1965, pp. 106-108.

[6] W. R. McCluney, "An Investigation of Subharmonic Generation in an Ultrasonic Resonant Cavity", M.S. Thesis, University of Tennessee, 1966. (Also published as Technical Report No. 2, AD 641 604, Office of Naval Research.)

[7] M. A. Breazeale and W. R. McCluney, "Subharmonic Generation in an Ultrasonic Resonant Cavity", J. Acoust. Soc. Am. 40, November, 1966, p. 1262.

[8] C. V. Raman and N. S. N. Nath, "The Diffraction of Light by High Frequency Sound Waves: Part II", Proc. Indian Acad. Sci., 2, 1935, 413-420.

[9] W. G. Mayer, "Reflection and Refraction of Mechanical Waves at Solid-Liquid Boundaries. II", J. Appl. Phys. 34, November, 1963, pp. 3286-3288.

[10] W. Keck and R. T. Beyer, "Frequency Spectrum of Finite Amplitude Ultrasonic Waves in Liquids", Phys. Fluids, 3, May-June, 1960, pp. 346-347.

[11] B. D. Cook and E. A. Hiedemann, "Diffraction of Light by Ultrasonic Waves of Various Standing Wave Ratios", J. Acoust. Soc. Am., 33, July, 1961, pp. 945-948.

[12] W. R. Klein and B. D. Cook, to be published in IEEE Trans. on Sonics and Ultrasonics.